

## Structural features and pro-inflammatory effects of water-soluble organic matter in inhalable fine urban air particles

Antoine Simões Almeida, Rita Ferreira, Artur M. S. Silva,  
Armando C. Duarte, Bruno Neves, and Regina M.B.O. Duarte

*Environ. Sci. Technol.*, **Just Accepted Manuscript** • DOI: 10.1021/acs.est.9b04596 • Publication Date (Web): 11 Nov 2019

Downloaded from [pubs.acs.org](https://pubs.acs.org) on November 11, 2019

### Just Accepted

“Just Accepted” manuscripts have been peer-reviewed and accepted for publication. They are posted online prior to technical editing, formatting for publication and author proofing. The American Chemical Society provides “Just Accepted” as a service to the research community to expedite the dissemination of scientific material as soon as possible after acceptance. “Just Accepted” manuscripts appear in full in PDF format accompanied by an HTML abstract. “Just Accepted” manuscripts have been fully peer reviewed, but should not be considered the official version of record. They are citable by the Digital Object Identifier (DOI®). “Just Accepted” is an optional service offered to authors. Therefore, the “Just Accepted” Web site may not include all articles that will be published in the journal. After a manuscript is technically edited and formatted, it will be removed from the “Just Accepted” Web site and published as an ASAP article. Note that technical editing may introduce minor changes to the manuscript text and/or graphics which could affect content, and all legal disclaimers and ethical guidelines that apply to the journal pertain. ACS cannot be held responsible for errors or consequences arising from the use of information contained in these “Just Accepted” manuscripts.

1 Structural features and pro-inflammatory effects of  
2 water-soluble organic matter in inhalable fine urban  
3 air particles

4 *Antoine S. Almeida,<sup>1</sup> Rita M. P. Ferreira,<sup>2</sup> Artur M. S. Silva,<sup>2</sup> Armando C. Duarte,<sup>1</sup> Bruno*  
5 *M. Neves,<sup>3,§</sup> Regina M. B. O. Duarte<sup>1,§,\*</sup>*

6 <sup>1</sup> Department of Chemistry & CESAM, University of Aveiro, 3810-193 Aveiro, Portugal

7 <sup>2</sup> Department of Chemistry & QOPNA and LAQV-REQUIMTE, University of Aveiro, 3810-  
8 193 Aveiro, Portugal

9 <sup>3</sup> Department of Medical Sciences and Institute of Biomedicine – iBiMED, University of  
10 Aveiro, 3810-193 Aveiro, Portugal

11

12 *§ supervised this study equally as senior authors*

13

## 14 ABSTRACT

15 The impact of inhalable fine particulate matter (PM<sub>2.5</sub>, aerodynamic diameter < 2.5 μm) on public  
16 health is of great concern worldwide. Knowledge on their harmful effects are mainly due to studies  
17 carried out with whole air particles, being the contribution of their different fractions largely  
18 unknown. Herein, a set of urban PM<sub>2.5</sub> samples were collected during day and nighttime periods  
19 in Autumn and Spring, aiming to address the seasonal and day-night variability of water-soluble  
20 organic matter (WSOM) composition. *In vitro* analysis of oxidative and pro-inflammatory  
21 potential of WSOM samples was carried out in both acute (24 h) and chronic (3 weeks) exposure  
22 setups using Raw264.7 macrophages as cell model. Findings revealed that the structural  
23 composition of WSOM samples differs between seasons and in a day-night cycle. Cells  
24 exposure resulted in an increase in the transcription of the cytoprotective *Hmox1* and pro-  
25 inflammatory genes *I11b* and *Nos2*, leading to a moderate pro-inflammatory status. These  
26 macrophages showed an impaired capacity to subsequently respond to a strong pro-  
27 inflammatory stimulus such as bacterial lipopolysaccharide, which may implicate a  
28 compromised capacity to manage harmful pathogens. Further investigation on aerosol  
29 WSOM could help to constrain the mechanisms of WSOM-induced respiratory diseases  
30 and contribute to PM<sub>2.5</sub> regulations.

31

32

33

## 34 INTRODUCTION

35 Inhalable fine atmospheric particulate matter (PM<sub>2.5</sub>, aerodynamic diameter < 2.5 μm) is  
36 of serious concerns in terms of health effects, including cardiovascular diseases,<sup>1,2</sup> airway  
37 damages and lung carcinogenesis,<sup>2-4</sup> and adverse neurodevelopmental effects.<sup>5-7</sup>  
38 Oxidative stress, genotoxicity, and inflammation have been suggested to be the central  
39 mechanisms by which PM<sub>2.5</sub> may impair the normal cellular physiological/biochemical  
40 processes, resulting in tissues damages and, therefore, facilitating the incidence and  
41 development of those adverse health outcomes.<sup>2</sup> Lung cells, such as epithelial cells and  
42 alveolar macrophages, are the primary targets of PM<sub>2.5</sub>-induced oxidative damage and  
43 pro-inflammatory effects.<sup>8-10</sup> In the past, these effects have been linked to PM<sub>2.5</sub> mass  
44 concentration;<sup>9,11</sup> however, evidences indicate that PM<sub>2.5</sub> chemical composition play an  
45 important role in the interaction between fine particles and lung cells membrane.<sup>10,12-17</sup>  
46 PM<sub>2.5</sub> is a complex mixture of inorganic and carbonaceous constituents, whose  
47 composition depends on the emission sources (natural and/or anthropogenic), formation  
48 process (*i.e.*, secondary origin), atmospheric processing, and weather conditions. A small  
49 set of chemical species have been linked to the oxidative potential and inflammatory

50 impact of ambient PM<sub>2.5</sub>. These include water-soluble metals (*e.g.*, Fe, Ni, Cu, Cr, Mn,  
51 Zn, V, and Pb),<sup>10,12,17,18</sup> water-soluble ions (*e.g.*, SO<sub>4</sub><sup>2-</sup>, NO<sub>3</sub><sup>-</sup>),<sup>10</sup> solvent-extractable  
52 organic components, such as polycyclic aromatic hydrocarbons (PAHs) and PAH nitro-  
53 derivatives, polychlorinated biphenyls, organochlorine pesticides, and polybrominated  
54 diphenyl ethers,<sup>16,18,19</sup> and wood smoke tracers (*e.g.*, levoglucosan and galactosan).<sup>19,20</sup>  
55 Although not receiving much attention by the air pollution health research community,  
56 water-soluble organic matter (WSOM) of ambient PM<sub>2.5</sub> have been recently also  
57 recognized as capable of mediating reactive oxygen species (ROS) generation.<sup>17,21–26</sup> In  
58 Northern Hemisphere midlatitudes, this organic aerosol component represent 10 to 80%  
59 of the total particulate organics,<sup>27–30</sup> whereas lower percentage values (up to 13%) have  
60 been reported for Southern Hemisphere locations.<sup>31</sup> Based on highly informative off-line  
61 analytical techniques, such as multidimensional nuclear magnetic resonance (NMR)  
62 spectroscopy and high-resolution mass spectrometry, it has been shown that aerosol  
63 WSOM consists of a highly diverse suite of oxygenated compounds, including  
64 dicarboxylic acids, keto-carboxylic acids, aliphatic aldehydes and alcohols, saccharides,  
65 saccharide anhydrides, aromatic acids, phenols, but also amines, amino acids, organic

66 nitrates, and organic sulfates.<sup>31–40</sup> Although being a major fraction of organic aerosols,  
67 the way by which the aerosol WSOM is redox-active or exert inflammation remains  
68 unresolved. It contributes greatly to this situation the inherent complexity of aerosol  
69 WSOM, with different chemical structures and associated physical properties. The use of  
70 chemical assays, such as dithiothreitol (DTT), has suggested important contributions of  
71 specific aerosol WSOM fractions, namely of isolated hydrophobic fractions (the so-called  
72 “humic-like substances” operational concept),<sup>21,22,25</sup> on the oxidative potential of ambient  
73 PM<sub>2.5</sub>. However, no evidence exists on which structural components of aerosol WSOM  
74 actually induce oxidative stress and inflammation. An enhanced knowledge of the relative  
75 contribution of WSOM substructures to the oxidative and pro-inflammatory potential of  
76 this organic aerosol fraction would be useful to understand the net impacts of air  
77 particulate organic matter on human health.

78 Within this context, this study aims to establish a relationship between the oxidative and  
79 pro-inflammatory potential of aerosol WSOM and their atmospheric concentrations and  
80 structural characteristics. A set of PM<sub>2.5</sub> samples were collected at an urban location,  
81 during day and nighttime periods, in Autumn and Spring seasons. With this PM<sub>2.5</sub>

82 sampling scheme, it was intended to apportion the seasonal and day-night variability of  
83 WSOM structures to their oxidative and pro-inflammatory potential. The compositional  
84 features of aerosol WSOM samples were exploited by liquid-state one-dimensional (1D)  
85 and two-dimensional (2D) NMR spectroscopy. The effects of aerosol WSOM on nitric  
86 oxide (NO) production, ROS cellular levels, transcription of the inflammatory genes *I1b*  
87 and *Nos2*, as well as activation of associated signalling pathway NF-κB were assessed  
88 in Raw264.7 macrophages. The effect on the transcription levels of *Hmox1*, a central  
89 player in detoxification of electrophilic and oxidative stresses, was also evaluated. The  
90 biological assays were carried out considering the effect of both acute (24 h) and chronic  
91 (3 weeks) exposures to aerosol WSOM, with the latter at maximal theoretical WSOM  
92 doses (*i.e.*, considering the average human air intake per hour, and the atmospheric  
93 water-soluble organic carbon concentrations in day-night cycles). Investigating the  
94 potential impact of aerosol WSOM composition on human health is essential, particularly  
95 when experiencing serious pollution conditions. This study set the basis for further  
96 understanding of the mechanisms of fine aerosol WSOM-induced respiratory diseases  
97 and may contribute to the development of targeted PM<sub>2.5</sub> regulations.



98

99

## 100 MATERIALS AND METHODS

### 101 Aerosol sampling and extraction of WSOM samples

102 The PM<sub>2.5</sub> samples were collected on a rooftop (*c.a.* 20 m above the ground) at the  
103 campus of University of Aveiro (40°38'N, 8°39'W), which is located about 10 km from the  
104 Atlantic coast on the outskirts of the city of Aveiro. The sampling site is impacted by both  
105 marine air masses travelling from the Atlantic Ocean and anthropogenic emissions from  
106 vehicular transport, residential, and industrial sources.<sup>30,32,41</sup> Episodes of increased PM<sub>2.5</sub>  
107 and WSOM concentrations are common in this area during colder periods and they can  
108 last several days,<sup>29,30,41</sup> allowing the collection of enough amount of aerosol WSOM within  
109 relatively short periods of time. The PM<sub>2.5</sub> samples were collected from 14 to 29  
110 November 2016 (Autumn) and 27 March to 04 April 2016 (Spring), during the weekdays  
111 (*i.e.*, from Monday to Friday) in two distinct time periods: (i) daytime: 9:40 a.m. to 5:30  
112 p.m. (Autumn)/6:30 p.m. (Spring), and (ii) overnight: 5:40 p.m. (Autumn)/6:40 p.m.  
113 (Spring) to 9:30 a.m. The PM<sub>2.5</sub> samples were collected on pre-fired quartz-fiber filters

114 (20.3×25.4 cm; Whatman QM-A) with an airflow rate of 1.13 m<sup>3</sup> min<sup>-1</sup>. Additional details  
115 on aerosol sampling procedure are available in Section S1, in Supporting Information (SI).  
116 After sampling, the filter samples were folded in two, wrapped in aluminum foil and  
117 immediately transported to the laboratory, where they were weighted and stored frozen  
118 until further analysis. The meteorological data recorded during PM<sub>2.5</sub> collection is  
119 available in Table S1 (SI). The determination of organic carbon (OC) and elemental  
120 carbon (EC) in each PM<sub>2.5</sub> sample was performed by means of a Lab OC-EC Aerosol  
121 Analyzer (Sunset Laboratory Inc.) following a thermo-optical method, described in section  
122 S2 (SI).

123 An area of 315 cm<sup>2</sup> of each quartz filter was extracted with 150 mL of ultra-pure water  
124 (18.2 MΩ cm, filter area to water volume ratio of 2.1 cm<sup>2</sup> mL<sup>-1</sup>) by mechanical stirring for  
125 5 min followed by ultrasonic bath for 15 min. Each final aqueous slurry was filtered through  
126 a hydrophilic polyvinylidene fluoride membrane filter (Durapore®, Millipore, Ireland) of  
127 0.22 μm pore size. At the end of this filtration step, the slurry residue was washed twice  
128 with 20 mL of ultrapure water in order to remove any water-soluble organic carbon  
129 (WSOC) still loosely bound to the filter residues. The dissolved organic carbon content of

130 each aqueous extract was measured by means of a Skalar (Breda, Netherlands) San++  
131 Automated Wet Chemistry Analyzer, based on a UV-persulfate oxidation method.<sup>42</sup>  
132 After the WSOC extraction, and to obtain sufficient amount of WSOM samples for both  
133 NMR and biological assay studies, the aqueous aerosol extracts from each sampling  
134 period within each season were batched together, on a total of four pooled WSOM  
135 samples representative of day and nighttime conditions in Autumn and Spring seasons.  
136 Each pooled WSOM sample was further divided into two aliquots of similar volume: one  
137 aimed to NMR analysis and the other to biological assay studies. The aliquots were  
138 freeze-dried, and the obtained residues (designated as “whole aerosol WSOM sample”)  
139 were kept in a desiccator over silica gel until further analysis. Additional details on aerosol  
140 WSOM samples processing are available in Figure S1, section S3 (SI).

141

#### 142 **Liquid-state 1D and 2D NMR spectroscopy**

143 All NMR spectra were acquired using a Bruker Avance-500 spectrometer operating at  
144 500.13 and 125.77 MHz for  $^1\text{H}$  and  $^{13}\text{C}$ , respectively, and equipped with a liquid nitrogen  
145 cooling CryoProbe Prodigy™. All 1D and 2D spectra were run at 295.1 K, and additional

146 details on NMR data acquisition can be found in Section S4, in SI. The dried WSOM  
147 samples (7 to 3 mg) were dissolved in deuterated methanol ( $\text{MeOH-}d_4$ , ~1 mL) and  
148 transferred to 5 mm NMR tubes. The identification of functional groups in the NMR spectra  
149 was based on their chemical shift relative to solvent ( $\text{MeOH-}d_4$ ) peak set at  $\delta_{\text{H}}$  3.31 ppm  
150 and  $\delta_{\text{C}}$  49.0 ppm. The interpretation of the spectral regions and structural assignments  
151 were based on the NMR chemical shift data described in the literature for standard  
152 organic compounds and for natural organic matter from different environmental  
153 matrices,<sup>28,32,34,43,44</sup> as well as on data generated by NMR simulators software's and  
154 databases (namely, Perkin Elmer ChemBioDraw® Ultra 14.0 and nmrdb.org).<sup>45</sup>

155

## 156 **Cell culture and treatments**

157 Raw 264.7, a mouse leukaemic monocyte macrophage cell line from American Type  
158 Culture Collection (ATCC number: TIB-71), was cultured in Dulbecco's Modified Eagle  
159 Media (DMEM) supplemented with 10% non-inactivated fetal bovine serum, 100 U mL<sup>-1</sup>  
160 of penicillin, and 100  $\mu\text{g mL}^{-1}$  streptomycin at 37°C in a humidified atmosphere of 95% air  
161 and 5% CO<sub>2</sub>. For acute exposure experiments (4 to 24 h) cells were plated, let stabilize

162 overnight and then treated with indicated WSOC concentrations. In prolonged exposure  
163 experiments the cells were treated for 21 days, twice a day, with maximal theoretical  
164 inhaled doses of WSOC calculated from an mean inspired air volume of 8.64 m<sup>3</sup> per day:  
165 for Autumn season experiments, the cells were treated in the morning with 7.8 µg of  
166 daytime WSOC extract, and at the evening with 16.2 µg of nighttime extract; in Spring  
167 season experiments, the cells were treated in the morning with 5.6 µg of daytime WSOC  
168 extract and at the evening with 6.1 µg of nighttime extract. The cell treatments in the  
169 morning and evening were timed to mimic the schedule of PM<sub>2.5</sub> samples collection,  
170 whereas the cell medium was completely replaced every 2 days.

171

## 172 **Nitric oxide (NO) production and *in vitro* antioxidant activity**

173 The production of NO was measured by the accumulation of nitrite in the culture  
174 supernatants, using a colorimetric reaction with the Griess reagent as previously  
175 described.<sup>46</sup> In some of the experiments, it was assessed whether exposure to WSOM  
176 extracts affects the capacity of macrophages to respond to the strong pro-inflammatory  
177 stimuli bacterial LPS. In acute exposure experiments cells were pre incubated for 1 h with

178 WSOM extracts and then  $1 \mu\text{g mL}^{-1}$  LPS was added following an incubation period of 24  
179 h. In prolonged exposure experiments cells were treated for 21 days with WSOM extracts  
180 and then stimulated for additional 24h with  $1 \mu\text{g mL}^{-1}$  LPS. The effect of WSOM extracts  
181 on the modulation of LPS-induced cellular oxidative stress was also addressed. Briefly,  
182 Raw cells were plated at  $0.05 \times 10^6$  per well in a  $\mu$ -Chamber slide (IBIDI GmbH,  
183 Germany), allowed to stabilize overnight and then stimulated with  $1 \mu\text{g mL}^{-1}$  LPS during  
184 24 h. The WSOM extracts were added 1 h prior to LPS stimulation. At the end of  
185 incubation period, cells were washed three times and then loaded with  $5 \mu\text{M}$   $\text{H}_2\text{DCFDA}$   
186 and  $0.5 \mu\text{g mL}^{-1}$  Hoechst in Hank's Balanced Salt Solution (HBSS) for 30 min at  $37^\circ\text{C}$  in  
187 the dark. Cells were washed three times with HBSS and analyzed with an Axio Observer  
188 Z1 fluorescent microscope (Zeiss Group, Oberkochen, Germany) at 63X magnification.

189

#### 190 **Analysis of gene expression by q-PCR**

191 After cell treatment for the indicated times, total RNA was isolated with TRIzol reagent  
192 according to the manufacturer's instructions. For analysis of mRNA levels of selected  
193 genes,  $1 \mu\text{g}$  of total RNA was reverse-transcribed using the iScript Select cDNA Synthesis

194 Kit and then real-time quantitative PCR (qPCR) reactions were performed using SYBR  
195 Green on a Bio-Rad CFX Connect device. The results were normalized using *Hprt1* as  
196 reference gene and presented as fold change relatively to untreated cells. Primer  
197 sequences were designed using Beacon Designer software version 8 (Premier Biosoft  
198 International, Palo Alto, CA, USA) and thoroughly tested.

199

## 200 **Statistical analysis**

201 Since aerosol WSOM samples were pooled and analyzed together, it should be  
202 mentioned that the cellular responses and PCR data were obtained for each pooled  
203 WSOM sample. However, at least three independent biological experiments were carried  
204 out for each sample. Results are presented as mean  $\pm$  the standard deviation (SD) of the  
205 indicated number of experiments. Comparisons between two groups were made by the  
206 two-sided unpaired Student's *t* test and multiple group comparisons by One-Way ANOVA  
207 analysis, with a Dunnett's Multiple Comparison post-test. Statistical analysis was  
208 performed using GraphPad Prism, version 6 (GraphPad Software, San Diego, CA, USA).  
209 Significance levels are as follows: \* $p < 0.05$ , \*\* $p < 0.01$ , \*\*\* $p < 0.001$ , \*\*\*\* $p < 0.0001$ .

210

211

**212 RESULTS AND DISCUSSION****213 Water-solubility of fine urban organic aerosols**

214 The ambient concentrations of PM<sub>2.5</sub>, OC, EC, and WSOC follow the same seasonal  
215 trend, with the highest levels being found during Autumn (Table 1, and Figures S2 to S5  
216 in SI). This seasonal trend has been quite well documented in this and other  
217 regions,<sup>28,30,33,37</sup> although an opposite trend has been observed in North America.<sup>47,48</sup> In  
218 Autumn, the median PM<sub>2.5</sub> concentration increased 1.5 fold during nighttime compared  
219 with daytime, which is likely due to a lower mixing height and more stable atmospheric  
220 conditions during the nighttime as well as increased emissions from residential heating  
221 sources. These events could also explain the 3.3 and 3.6 fold increase in OC and WSOC  
222 concentrations, respectively, during nighttime. In Spring, the diurnal variations of the  
223 median OC and WSOC concentrations were evident, but the median concentration values  
224 of these carbonaceous fractions only increased 1.3 and 1.5 fold, respectively, during  
225 nighttime, whereas no major difference was observed for the PM<sub>2.5</sub> levels. Interestingly,



226 the OC-day/OC-night, EC-day/EC-night, and WSOM-day/WSOM-night ratios increased  
227 from a range of 0.34 – 0.71, 0.14 – 0.72, and 0.40 – 0.65, respectively, between the 27<sup>th</sup>  
228 and 29<sup>th</sup> of March, to 1.2 – 2.7, 0.8 – 1.8, and 1.1 – 2.1, respectively, between 30<sup>th</sup> of  
229 March and 6<sup>th</sup> of April (Figures S3 to S5, SI). This increase could be explained by a  
230 decrease in the OC, EC and WSOC concentrations during nighttime in the second half of  
231 the sampling period. During this period, the median values of temperature and maximum  
232 wind velocity raised from 13 to 15°C and 2.7 to 4.0 m s<sup>-1</sup>, respectively, leading to a more  
233 turbulent atmosphere and less emissions from anthropogenic activities related to house  
234 heating and, therefore, to a decrease in the nighttime OC, EC and WSOC concentrations.  
235 Furthermore, it is also likely that an additional OC source was present in daytime Spring  
236 samples, which cannot be explained solely by changes in primary emissions in view of  
237 the decrease of EC concentrations compared with Autumn. Considering that photo-  
238 oxidative capacity of atmosphere might be enhanced in Spring,<sup>28,29</sup> *in situ* production of  
239 secondary OC or chemical aging of insoluble primary organics could likely contribute to  
240 this additional OC. This enhanced photochemical activity can also explain the higher  
241 WSOC/OC ratios of Spring samples compared to those of Autumn samples.

242 <TABLE 1 here>

243

244 **Day-night variability of aerosol WSOM features**

245 Figure 1(A) shows the  $^1\text{H}$  NMR spectra of pooled aerosol WSOM samples representative  
246 of day and nighttime conditions in Autumn and Spring seasons. These  $^1\text{H}$  NMR spectra  
247 exhibit a remarkable similarity to those of other urban aerosol WSOM samples,<sup>28,30-32</sup>  
248 comprising a complex overlapping profile with broad bands superimposed by a relatively  
249 small number of sharp peaks. For a further understanding of these spectral profiles, a  
250 quantitative integration of the four main regions assigned to different types of non-  
251 exchangeable organic hydrogen [Figure 1(A)] was performed in order to assess the  
252 abundance of each functionality in WSOM samples. As depicted in Figure 1(B), and  
253 regardless of the sampling period, the saturated aliphatic protons (H-C) are typically the  
254 most important component, followed by unsaturated (H-C=C=) and oxygenated (H-C-O)  
255 aliphatic protons, and a less contribution from aromatic protons (Ar-H). Comparison  
256 between daytime and nighttime WSOM samples are expected to vary somewhat within  
257 both seasons, due to the distinctly different emission sources and atmospheric oxidation

258 conditions. However, in Spring, very little day-night variability was observed for the NMR  
259 structural signatures identified in the WSOM samples. On the other hand, in Autumn, the  
260 aliphatic H–C structures exhibit a distinct maximum (45%) for day aerosol WSOM and a  
261 minimum (34%) for the night sample. Additional differences between day and night  
262 WSOM samples in Autumn are found in the spectral regions associated with protons  
263 bound to oxygenated aliphatic (H–C–O) and aromatic (Ar–H) structures, whose  
264 contributions are higher for WSOM collected overnight (29% and 11%, respectively) than  
265 in WSOM collected in daytime (19% and 6.8%, respectively). The occurrence of strong  
266 H–C–O and aromatic signatures overnight in Autumn may be associated with the  
267 contribution of fresh biomass burning emissions for house heating under low air  
268 temperature conditions.<sup>28,30,31</sup> Moreover, the presence of an intense sharp resonance at  
269  $\delta$  <sup>1</sup>H 5.3 ppm [Figure 1(A)] attributed to protons bound to anomeric carbons [O–C(H)–O],  
270 such as those of anhydrosugars (e.g., levoglucosan and mannosan), which are known  
271 molecular markers of wood burning emissions,<sup>30,32</sup> further confirms the presence of  
272 smoke particles during this period.

273 <FIGURE 1 here>

274 The compositional day-night variability of aerosol WSOM samples within the two seasonal  
275 periods were further ascertain using 2D NMR spectroscopy (Figures S6 to S8, in SI). The  
276  $^1\text{H}$ - $^{13}\text{C}$  HSQC NMR spectra of all WSOM samples reveal several important  $^1\text{H}$ - $^{13}\text{C}$   
277 correlations in three major regions of chemical environments (Figures S6 and S7), but  
278 with very different relative intensities: aliphatic ( $\delta_{\text{H}}$  0.4–3.6 ppm/ $\delta_{\text{C}}$  10–45 ppm,  
279 represented by H–C and H–C–C=), *O*-alkyl ( $\delta_{\text{H}}$  3.6–6.0 ppm/ $\delta_{\text{C}}$  50–107 ppm, including  
280 anomeric carbons), and aromatic ( $\delta_{\text{H}}$  6.5–8.5 ppm/  
281  $\delta_{\text{C}}$  107–160 ppm) regions. The structural assignments of the 2D NMR cross peaks within  
282 these three chemical shift areas were further carried out based on spectral data from  
283 previous 2D NMR studies of aerosol WSOM samples.<sup>30,32,34,49</sup> The main structural  
284 findings are shown in the expanded aliphatic, *O*-alkyl, and aromatic regions of the  $^1\text{H}$ - $^{13}\text{C}$   
285 HSQC NMR spectra in Figures S9 to S20 in SI. Overall, 15 polyfunctional aliphatic and  
286 aromatic substructures were identified in this study as being common to all aerosol  
287 WSOM samples, whereas 4 aromatic substructures were typical of aerosol WSOM  
288 sample collected overnight in Autumn (Figure S21, in SI). The presence of these 4 typical  
289 aromatic substructures [structures (18) to (21) in Figure S21] in overnight Autumn WSOM

290 sample confirm the notable influence of biomass burning emissions into the aerosol  
291 WSOM characteristics during this period.<sup>30,32</sup> Five carbohydrate-like structures [structures  
292 (11) to (15), in Figure S21] were consistently found in all aerosol WSOM samples, but  
293 particularly more prominent in samples collected overnight in Autumn. Except for  
294 trehalose [structure (13) in Figure S21], usually referred as a tracer for the resuspension  
295 of surface soil and unpaved road dust,<sup>50</sup> the presence of the anhydrosugars levoglucosan  
296 and mannosan [structures (11) and (12), respectively, Figure S21] and disaccharides  
297 maltose and sucrose [structures (14) and (15), respectively, Figure S21] further confirm  
298 that biomass burning is an important contributor to aerosol WSOM collected overnight in  
299 Autumn.<sup>30,32</sup> The presence in all WSOM samples of NMR fingerprints assigned to DMA<sup>+</sup>,  
300 DEA<sup>+</sup> and MSA [structures (7) to (9) in Figure S21], and terephthalic acid [structure (16)  
301 in Figure S21] also pinpoint to the contribution of, respectively, marine organic aerosols<sup>30</sup>  
302 and oxidized aromatic hydrocarbons from urban traffic emissions<sup>30,32</sup> to aerosol WSOM  
303 samples. Despite relatively uniform seasonal distribution of aliphatic structures among all  
304 aerosol WSOM samples, there are actually important differences in the aromatic and *Q*-  
305 alkyl composition of nighttime aerosol WSOM samples in Autumn [summarized in Figure

306 1(C)]. These differences in WSOM chemical composition are expected to exert dissimilar  
307 contribution on the oxidative and pro-inflammatory effects of air organic particles.

### 308 **Cytotoxicity of aerosol WSOM and impact on macrophages ROS and NO production**

309 Understanding the interaction between airway cellular populations and atmospheric air  
310 particles, as well as the mechanisms through which their constituents cause inflammation  
311 and cellular redox imbalances is of major importance. Therefore, the cytotoxicity of  
312 aerosol WSOM over macrophages was firstly assessed in the WSOC concentration range  
313 of 1 to 100  $\mu\text{g mL}^{-1}$ , allowing to conclude that none caused a significant decrease in cell  
314 viability (Section S7, Figure S22). Treatments with LPS or LPS + WSOM are also devoid  
315 of significant impact on macrophages viability (Section S7, Figure S23). As NO is a key  
316 molecule in inflammation and to the macrophage capacity to destroy invading pathogens,  
317 the ability of WSOM to induce NO production and to modulate the LPS-induced  
318 production in these cells was also analyzed. As shown in Figure S24(A), Section S8, day  
319 and night WSOM Autumn samples at higher concentrations slightly induce NO  
320 production. This is in agreement with previous reports showing small increases in NO  
321 release by macrophages treated with particle or water-soluble fraction of  $\text{PM}_{2.5}$ .<sup>51,52</sup>

322 Furthermore, it can be perceived a different trend between the two WSOM samples: while  
323 the day Autumn WSOM extract causes a concentration dependent increase in NO  
324 production, the night extract has an opposite behavior. We hypothesize that the night  
325 Autumn WSOM may contain organic compounds that induce NO, but also other  
326 constituents that counteract this effect. Regarding the effects of Spring WSOM samples,  
327 only day samples significantly induce NO release [Figure S24(A)]. Discrepancies between  
328 the biological effects of PM<sub>2.5</sub> and its WSOM fraction collected during day or night are still  
329 poorly documented, but the impact of seasonal variations in PM<sub>2.5</sub> chemical composition  
330 (*e.g.* inorganic ions, elements and PAHs) and cytotoxicity has been extensively  
331 covered.<sup>53–55</sup>

332 Interestingly, the effects of WSOM samples on the LPS-induced NO production was  
333 significantly inhibited by all the samples at the concentration of 75 µg mL<sup>-1</sup> [Figure  
334 S24(B)]. This effect was not due to a direct NO scavenging activity (Figure S25), but  
335 instead it may be the result of a modulation of inducible nitric oxide synthase (iNOS)  
336 activity or gene transcription. Additionally, WSOM samples *per se* do not induced  
337 oxidative stress, and surprisingly were able to markedly inhibit the LPS-triggered ROS

338 production in treated macrophages (Figure 2). These results differ from several reports  
339 where atmospheric particulate matter (PM) were shown to exert pro-oxidative effects.<sup>17,56–</sup>  
340 <sup>58</sup> These discrepancies may be explained by the differences in the material actually used  
341 since most of the available studies employ the whole air PM, or instead it could be due to  
342 considerable differences in the chemical composition of WSOM samples. The pro-  
343 oxidative characteristics of PM can be therefore mainly attributed to direct physical  
344 interactions with the particles themselves, or to their content in elements such as Cu, Cr,  
345 Pb, Co, Ni, or even WSOC.<sup>17,58</sup> It should be mentioned that the concentration of water-  
346 soluble elements and metals in the aqueous PM<sub>2.5</sub> extracts here studied are lower than  
347 those identified in the literature as exerting biological effects (Section S9, Table S2), thus  
348 supporting the assumption that the effects observed in this work are mainly due to an  
349 exposure to aerosol WSOM.

350 <FIGURE 2 here>

351 The inhibitory effect on the capacity of macrophages to produce ROS reported in this  
352 study is paradoxical: it may be beneficial given that it limits an inflammatory reaction;



353 however, it can compromise the efficacy of macrophages to destroy harmful  
354 microorganisms during an infection by limiting the oxidative burst.

355

356

### 357 **Effects of aerosol WSOM on the modulation of macrophage inflammatory status**

358 Based on the results obtained thus far, the potential anti-inflammatory activity of aerosol  
359 WSOM samples was also explored. For this, the impact of WSOM samples on the  
360 transcription of *Il1b*, *Nos2* (pro-inflammatory genes) and *Hmox1* (anti-  
361 inflammatory/cytoprotective), or in the modulation of their LPS-induced transcription was  
362 evaluated. As shown in Figure S26, Section S10, Autumn and Spring WSOM samples  
363 present a similar profile, although with different magnitudes. *Hmox1* transcription is  
364 induced either by day or night samples in a dose dependent way. This observation agrees  
365 with previous reports where PAHs present in PM (fine and coarse) were shown to induce  
366 *Hmox1* transcription.<sup>2,59,60</sup> *Hmox* is a detoxifying enzyme that is expressed in response to  
367 oxidative and electrophilic stresses as the result of the activation of the Keap/Nrf2  
368 signaling pathway.<sup>61</sup> Therefore, the observed increases indicate that WSOM samples contain

369 electrophilic compounds, of which substructures (1) and (8) to (10) in Figure 1(C) might be  
370 suitable candidates.

371 Regarding the modulation of *I1b* and *Nos2* transcription, once again Autumn and Spring  
372 WSOM samples presented a similar profile, with moderate increases being induced  
373 (Figure S26). These results are in agreement with previous studies where the exposure  
374 to PM<sub>2.5</sub> was shown to increase the transcription of *I1b* and *Nos2* genes in the same cell  
375 model, causing a moderate pro-inflammatory effect.<sup>60,62</sup> In this study, when comparing  
376 day and night WSOM samples, there are clear differences: while for day WSOM, the  
377 increase in samples concentration is followed by an increase in the transcription of  
378 referred genes, the opposite occurs for night samples (Figure S26). This explains the  
379 lower production of NO in cells treated with higher concentrations of night WSOM  
380 samples [Figure S24(A)]. Regarding the cells treated with LPS, although all the tested WSOM  
381 samples have slight pro-inflammatory properties, they downregulate the LPS-induced  
382 inflammatory state by increasing *Hmox1* and reducing *I1b* and *Nos2* transcription (Figure 3).  
383 Similar profiles were found when the levels of these proteins were analyzed by western blot  
384 (Section S11, Figure S27). The increase in *Hmox1* transcription and respective protein expression  
385 in addition to the intrinsic antioxidant characteristics of the WSOM samples support their strong  
386 capacity to prevent LPS-induced oxidative stress. In turn, the decrease in the LPS-induced *Nos2*

387 transcription (Figures 3) resulted in a downregulation of the iNOS protein levels (Figure S27),  
388 which can explain the observed decrease of LPS-induced NO production in cells pre-treated with  
389 WSOM extracts. This capacity to limit LPS-induced inflammatory status was not due to  
390 impairment of NF- $\kappa$ B nuclear translocation (Section S12, Figure S28). Given that MAPKs  
391 signaling pathways were also shown to modulate PM-induced inflammation,<sup>63,64</sup> the effects of  
392 WSOM extracts on the phosphorylation levels of p38, JNK and ERK (Section S13, Figure S29)  
393 were also assessed. While ERK was not affected and JNK marginally activated, LPS-induced  
394 activation of p38MAPK signaling cascade was downmodulated by exposure to extracts,  
395 particularly to nighttime WSOM samples (Figure S29). This impairment of p38 MAPK activation  
396 may be in part responsible for the observed decrease in LPS-triggered inflammatory status.  
397 Additionally, contributing to this impaired capacity of macrophages to mount an adequate  
398 inflammatory response, the extracts may be causing alterations in the cellular cytoskeleton,  
399 impairing the traffic of secretory vesicles and the release of cytokines, in a process similar to the  
400 one recently described by Longhin and collaborators.<sup>65</sup>

401 <FIGURE 3 here>

402 Given that all experiments were performed with relatively high WSOC concentrations  
403 within an acute exposure setup, it was decided to analyze the effects of chronic exposure  
404 by culturing cells during 3 weeks with maximal theoretical aerosol WSOM doses. For this,  
405 the average human air intake per hour and the atmospheric WSOC concentrations during  
406 day and nighttime conditions were taken into account for administrating maximal

407 theoretical WSOC quantities in day-night cycles. As demonstrated in Figure 4(A), cells  
408 exposed to aerosol WSOM exhibit a slight increase in the transcription of *Hmox1*, *Il1b*,  
409 and *Nos2* genes. When these cells chronically exposed to WSOM samples were then  
410 treated with LPS, the *Hmox1* and *Nos2* slightly increased, but the mRNA levels of *Il1b*  
411 were significantly down modulated [Figure 4(B)]. While this small increase observed in  
412 *Nos2* transcription does not reach statistical significance it reveals an opposite tendency  
413 to the one observed in acute experiments. We hypothesize that this may be mainly due  
414 the highly different applied WSOC concentrations and to the presence in the extracts of  
415 pro and anti-inflammatory compounds. In acute experiments the concentration of  
416 compounds with anti-inflammatory properties may reach a level enough to impair LPS-  
417 triggered signaling pathways, namely those regulating *Nos2* transcription. In contrast, in  
418 prolonged exposure experiments, the cells were continuously treated with very low  
419 amounts of WSOM extracts and the compounds with pro-inflammatory properties may  
420 prime cells rendering them more responsive to posterior LPS stimulation. Therefore,  
421 prolonged exposure to even very small concentrations of water-soluble organic

422 compounds present in  $PM_{2.5}$ , can cause a decrease in the capacity of macrophages to  
423 respond to a subsequent inflammatory stimulus.

424 <FIGURE 4 here>

425 In summary, the set of data provided by 1D and 2D NMR analysis indicates that the fine  
426 aerosol WSOM samples hold similar functional groups; however, they differ in terms of  
427 their relative distribution both between seasons and in a day-night cycle. This study also  
428 highlights that the compositional features of aerosol WSOM samples correlates with their  
429 ability to induce a moderate inflammatory status in macrophages, which at long-term may  
430 compromise their capacity to mount an effective inflammatory response required to  
431 manage harmful pathogens. Therefore, continuous and prolonged exposure to aerosol  
432 water-soluble organic compounds could result in increased susceptibility to respiratory  
433 infections. For a better understanding of the overall ability of fine aerosol WSOM to exert  
434 pro-inflammatory effects, further studies should be conducted involving a larger data set  
435 of different WSOM samples, while effectively segregating the contributions from different  
436 WSOM constituents.

437

438

439 ASSOCIATED CONTENT

440 **Supporting Information.** Experimental procedure for PM<sub>2.5</sub> sampling, meteorological  
441 information collected during each sampling campaign, experimental details for OC and  
442 EC analysis, average ambient concentrations of the main aerosol carbon fractions, 2D  
443 NMR data acquisition and 2D NMR spectral assignments of the aerosol WSOM samples,  
444 water-soluble elements and metals concentrations in PM<sub>2.5</sub> samples, impact of aerosol  
445 WSOM samples on macrophages viability, NO production and scavenging activity,  
446 modulation of macrophage inflammatory status, protein levels of iNOS, HMOX1, and IL-  
447 1 $\beta$ , activation of pro-inflammatory NF- $\kappa$ B signaling pathways, and modulation of MAPKs  
448 signaling pathways. This material is available free of charge via the Internet at  
449 <http://pubs.acs.org>.

450

451

452

## 453 AUTHOR INFORMATION

454 **Corresponding Author**

455 \*E-mail: [regina.duarte@ua.pt](mailto:regina.duarte@ua.pt); Phone: +351 234 370 360.

456 **Author Contributions**

457 The manuscript was written through contributions of all authors and all authors have given  
458 approval to its final version. § Bruno M. Neves and Regina M.B.O. Duarte supervised this study  
459 equally as senior authors.

460 ORCID: Antoine S. Almeida: 0000-0002-4535-1213; Rita M.P. Ferreira: 0000-0002-6872-  
461 4051; Artur M.S. Silva: 0000-0003-2861-8286; Armando C. Duarte: 0000-0002-4868-  
462 4099; Bruno M. Neves: 0000-0001-7391-3124; Regina M.B.O. Duarte: 0000-0002-1825-  
463 6528.

464

465 **Notes**

466 The authors declare no competing financial interest.

467

468 **ACKNOWLEDGMENT**

469 Thanks are due to FCT/MCTES for the financial support to CESAM  
470 (UID/AMB/50017/2019), Organic Chemistry Research Unit (QOPNA,  
471 UID/QUI/00062/2019), and iBiMED (UID/BIM/04501/2013 and UID/BIM/04501/2019), and  
472 Portuguese NMR network, through national funds. FCT/MCTES is also acknowledged for  
473 an Investigator FCT Contract (IF/00798/2015). The Authors would like to acknowledge  
474 Catarina Leitão for her assistance on the western blot experiments.

475

476

## 477 REFERENCES

- 478 (1) Mills, N. L.; Donaldson, K.; Hadoke, P. W.; Boon, N. A.; MacNee, W.; Cassee, F.  
479 R.; Sandström, T.; Blomberg, A.; Newby, D. E. Adverse Cardiovascular Effects of  
480 Air Pollution. *Nat. Clin. Pract. Cardiovasc. Med.* **2009**, *6* (1), 36–44.
- 481 (2) Feng, S.; Gao, D.; Liao, F.; Zhou, F.; Wang, X. The Health Effects of Ambient PM2.5  
482 and Potential Mechanisms. *Ecotoxicol. Environ. Saf.* **2016**, *128*, 67–74.
- 483 (3) Li, R.; Zhou, R.; Zhang, J. Function of PM2.5 in the Pathogenesis of Lung Cancer  
484 and Chronic Airway Inflammatory Diseases. *Oncol. Lett.* **2018**, *15* (5), 7506–7514.



- 485 (4) Santibáñez-Andrade, M.; Quezada-Maldonado, E. M.; Osornio-Vargas, Á.;  
486 Sánchez-Pérez, Y.; García-Cuellar, C. M. Air Pollution and Genomic Instability: The  
487 Role of Particulate Matter in Lung Carcinogenesis. *Environ. Pollut.* **2017**, *229*, 412–  
488 422.
- 489 (5) Basagaña, X.; Esnaola, M.; Rivas, I.; Amato, F.; Alvarez-Pedrerol, M.; Forns, J.;  
490 López-Vicente, M.; Pujol, J.; Nieuwenhuijsen, M.; Querol, X.; Sunyer, J.  
491 Neurodevelopmental Deceleration by Urban Fine Particles from Different Emission  
492 Sources : A Longitudinal Observational Study. *Environ. Health Perspect.* **2016**, *124*  
493 (10), 1630–1636.
- 494 (6) Calderón-Garcidueñas, L.; Kulesza, R. J.; Doty, R. L.; Angiulli, A. D.; Torres-  
495 Jardón, R. Megacities Air Pollution Problems: Mexico City Metropolitan Area  
496 Critical Issues on the Central Nervous System Pediatric Impact. *Environ. Res.*  
497 **2015**, *137*, 157–169.
- 498 (7) Suades-González, E.; Gascon, M.; Guxens, M.; Sunyer, J. Air Pollution and  
499 Neuropsychological Development: A Review of the Latest Evidence. *Endocrinology*  
500 **2015**, *156* (10), 3473–3482.

- 501 (8) Gosset, P.; Aboukais, A.; Dagher, Z.; Shirali, P.; Ledoux, F.; Surpateanu, G.;
- 502 Garçon, G.; Courcot, D.; Puskaric, E. Pro-Inflammatory Effects of Dunkerque City
- 503 Air Pollution Particulate Matter 2.5 in Human Epithelial Lung Cells (L132) in Culture.
- 504 *J. Appl. Toxicol.* **2005**, *25* (2), 166–175.
- 505 (9) Sun, Q.; Chen, L. C.; Briazova, T.; Laing, S.; Zhang, K.; Wang, G.; Wang, A.; Gow,
- 506 A.; Zhang, C.; Chen, A. F.; Rajagopalan, S.; Chen, L. C.; Sun, Q.; Zhang, K.
- 507 Airborne Particulate Matter Selectively Activates Endoplasmic Reticulum Stress
- 508 Response in the Lung and Liver Tissues. *Am. J. Physiol. Physiol.* **2010**, *299* (4),
- 509 C736–C749.
- 510 (10) Liu, Q.; Baumgartner, J.; Zhang, Y.; Liu, Y.; Sun, Y.; Zhang, M. Oxidative Potential
- 511 and Inflammatory Impacts of Source Apportioned Ambient Air Pollution in Beijing.
- 512 *Environ. Sci. Technol.* **2014**, *48* (21), 12920–12929.
- 513 (11) Pope, C. A.; Dockery, D. W. Health Effects of Fine Particulate Air Pollution: Lines
- 514 That Connect. *J. Air Waste Manag. Assoc.* **2006**, *56* (6), 709–742.
- 515 (12) Visentin, M.; Pagnoni, A.; Sarti, E.; Pietrogrande, M. C. Urban PM<sub>2.5</sub> Oxidative
- 516 Potential: Importance of Chemical Species and Comparison of Two

- 517 Spectrophotometric Cell-Free Assays. *Environ. Pollut.* **2016**, *219*, 72–79.
- 518 (13) Huang, Q.; Zhang, J.; Peng, S.; Tian, M.; Chen, J.; Shen, H. Effects of Water  
519 Soluble PM<sub>2.5</sub> Extracts Exposure on Human Lung Epithelial Cells (A549): A  
520 Proteomic Study. *J. Appl. Toxicol.* **2014**, *34* (6), 675–687.
- 521 (14) Fang, T.; Verma, V.; T Bates, J.; Abrams, J.; Klein, M.; Strickland, J. M.; Sarnat, E.  
522 S.; Chang, H. H.; Mulholland, A. J.; Tolbert, E. P.; Russel, G. A.; Weber, J. R.  
523 Oxidative Potential of Ambient Water-Soluble PM<sub>2.5</sub> in the Southeastern United  
524 States: Contrasts in Sources and Health Associations between Ascorbic Acid (AA)  
525 and Dithiothreitol (DTT) Assays. *Atmos. Chem. Phys.* **2016**, *16* (6), 3865–3879.
- 526 (15) Cassee, F. R.; Héroux, M.-E.; Gerlofs-Nijland, M. E.; Kelly, F. J. Particulate Matter  
527 beyond Mass: Recent Health Evidence on the Role of Fractions, Chemical  
528 Constituents and Sources of Emission. *Inhal. Toxicol.* **2013**, *25* (14), 802–812.
- 529 (16) MohseniBandpi, A.; Eslami, A.; Shahsavani, A.; Khodagholi, F.; Alinejad, A.  
530 Physicochemical Characterization of Ambient PM<sub>2.5</sub> in Tehran Air and Its Potential  
531 Cytotoxicity in Human Lung Epithelial Cells (A549). *Sci. Total Environ.* **2017**, *593*,  
532 182–190.

- 533 (17) Saffari, A.; Daher, N.; Shafer, M. M.; Schauer, J. J.; Sioutas, C. Global Perspective  
534 on the Oxidative Potential of Airborne Particulate Matter: A Synthesis of Research  
535 Findings. *Environ. Sci. Technol.* **2014**, *48* (13), 7576–7583.
- 536 (18) Janssen, N. A. H.; Yang, A.; Strak, M.; Steenhof, M.; Hellack, B.; Gerlofs-Nijland,  
537 M. E.; Kuhlbusch, T.; Kelly, F.; Harrison, R.; Brunekreef, B.; Hoek, G.; Cassee, F.  
538 Oxidative Potential of Particulate Matter Collected at Sites with Different Source  
539 Characteristics. *Sci. Total Environ.* **2014**, *472*, 572–581.
- 540 (19) Risom, L.; Møller, P.; Loft, S. Oxidative Stress-Induced DNA Damage by Particulate  
541 Air Pollution. *Mutat. Res. Mol. Mech. Mutagen.* **2005**, *592* (1–2), 119–137.
- 542 (20) Saffari, A.; Daher, N.; Samara, C.; Voutsas, D.; Kouras, A.; Manoli, E.;  
543 Karagkiozidou, O.; Vlachokostas, C.; Moussiopoulos, N.; Shafer, M. M.; Schauer,  
544 J. J.; Sioutas, C. Increased Biomass Burning Due to the Economic Crisis in Greece  
545 and Its Adverse Impact on Wintertime Air Quality in Thessaloniki. *Environ. Sci.*  
546 *Technol.* **2013**, *47* (23), 13313–13320.
- 547 (21) Lin, P.; Yu, J. Z. Generation of Reactive Oxygen Species Mediated by Humic-like  
548 Substances in Atmospheric Aerosols. *Environ. Sci. Technol.* **2011**, *45* (24), 10362–

- 549 10368.
- 550 (22) Verma, V.; Rico-Martinez, R.; Kotra, N.; King, L.; Liu, J.; Snell, T. W.; Weber, R. J.
- 551 Contribution of Water-Soluble and Insoluble Components and Their
- 552 Hydrophobic/Hydrophilic Subfractions to the Reactive Oxygen Species-Generating
- 553 Potential of Fine Ambient Aerosols. *Environ. Sci. Technol.* **2012**, *46* (20), 11384–
- 554 11392.
- 555 (23) Samara, C. On the Redox Activity of Urban Aerosol Particles: Implications for Size
- 556 Distribution and Relationships with Organic Aerosol Components. *Atmosphere*
- 557 *(Basel)*. **2017**, *8* (10).
- 558 (24) Saffari, A.; Daher, N.; Shafer, M. M.; Schauer, J. J.; Sioutas, C. Seasonal and
- 559 Spatial Variation in Reactive Oxygen Species Activity of Quasi-Ultrafine Particles
- 560 (PM<sub>0.25</sub>) in the Los Angeles Metropolitan Area and Its Association with Chemical
- 561 Composition. *Atmos. Environ.* **2013**, *79*, 566–575.
- 562 (25) Verma, V.; Fang, T.; Xu, L.; Peltier, R. E.; Russell, A. G.; Ng, N. L.; Weber, R. J.
- 563 Organic Aerosols Associated with the Generation of Reactive Oxygen Species
- 564 (ROS) by Water-Soluble PM<sub>2.5</sub>. *Environ. Sci. Technol.* **2015**, *49* (7), 4646–4656.

- 565 (26) Dou, J.; Lin, P.; Kuang, B. Y.; Yu, J. Z. Reactive Oxygen Species Production  
566 Mediated by Humic-like Substances in Atmospheric Aerosols: Enhancement  
567 Effects by Pyridine, Imidazole, and Their Derivatives. *Environ. Sci. Technol.* **2015**,  
568 *49*(11), 6457–6465.
- 569 (27) Zhang, Q.; Jimenez, J. L.; Canagaratna, M. R.; Allan, J. D.; Coe, H.; Ulbrich, I.;  
570 Alfarra, M. R.; Takami, A.; Middlebrook, A. M.; Sun, Y. L.; Dzepina, K.; Dunlea, E.;  
571 Docherty, K.; DeCarlo, P. F.; Salcedo, D.; Onasch, T.; Jayne, J. T.; Miyoshi, T.;  
572 Shimono, A.; Hatakeyama, S.; Takegawa, N.; Kondo, Y.; Schneider, J.; Drewnick,  
573 F.; Borrmann, S.; Weimer, S.; Demerjian, K.; Williams, P.; Bower, K.; Bahreini, R.;  
574 Cottrell, L.; Griffin, R. J.; Rautiainen, J.; Sun, J. Y.; Zhang, Y. M.; Worsnop, D. R.  
575 Ubiquity and Dominance of Oxygenated Species in Organic Aerosols in  
576 Anthropogenically-Influenced Northern Hemisphere Midlatitudes. *Geophys. Res.*  
577 *Lett.* **2007**, *34*(13).
- 578 (28) Lopes, S. P.; Matos, J. T. V.; Silva, A. M. S.; Duarte, A. C.; Duarte, R. M. B. O. 1 H  
579 NMR Studies of Water- and Alkaline-Soluble Organic Matter from Fine Urban  
580 Atmospheric Aerosols. *Atmos. Environ.* **2015**, *119*, 374–380.

- 581 (29) Duarte, R. M. B. O.; Freire, S. M. S. C.; Duarte, A. C. Investigating the Water-  
582 Soluble Organic Functionality of Urban Aerosols Using Two-Dimensional  
583 Correlation of Solid-State  $^{13}\text{C}$  NMR and FTIR Spectral Data. *Atmos. Environ.* **2015**,  
584 *116*, 245–252.
- 585 (30) Duarte, R. M. B. O.; Piñeiro-Iglesias, M.; López-Mahía, P.; Muniategui-Lorenzo, S.;  
586 Moreda-Piñeiro, J.; Silva, A. M. S.; Duarte, A. C. Comparative Study of Atmospheric  
587 Water-Soluble Organic Aerosols Composition in Contrasting Suburban  
588 Environments in the Iberian Peninsula Coast. *Sci. Total Environ.* **2019**, *648*, 430–  
589 441.
- 590 (31) Duarte, R. M. B. O.; Matos, J. T. V.; Paula, A. S.; Lopes, S. P.; Pereira, G.;  
591 Vasconcellos, P.; Gioda, A.; Carreira, R.; Silva, A. M. S.; Duarte, A. C.; Smichowski,  
592 P.; Rojas, N.; Sanchez-Ccoyllo, O. Structural Signatures of Water-Soluble Organic  
593 Aerosols in Contrasting Environments in South America and Western Europe.  
594 *Environ. Pollut.* **2017**, *227*, 513–525.
- 595 (32) Matos, J. T. V.; Duarte, R. M. B. O.; Lopes, S. P.; Silva, A. M. S.; Duarte, A. C.  
596 Persistence of Urban Organic Aerosols Composition: Decoding Their Structural

- 597 Complexity and Seasonal Variability. *Environ. Pollut.* **2017**, *231*, 281–290.
- 598 (33) Duarte, R. M. B. O.; Santos, E. B. H.; Pio, C. A.; Duarte, A. C. Comparison of  
599 Structural Features of Water-Soluble Organic Matter from Atmospheric Aerosols  
600 with Those of Aquatic Humic Substances. *Atmos. Environ.* **2007**, *41*, 8100–8113.
- 601 (34) Duarte, R. M. B. O.; Silva, A. M. S.; Duarte, A. C. Two-Dimensional NMR Studies  
602 of Water-Soluble Organic Matter in Atmospheric Aerosols. *Environ. Sci. Technol.*  
603 **2008**, *42* (22), 8224–8230.
- 604 (35) Ng, N. L.; Canagaratna, M. R.; Zhang, Q.; Jimenez, J. L.; Tian, J.; Ulbrich, I. M.;  
605 Kroll, J. H.; Docherty, K. S.; Chhabra, P. S.; Bahreini, R.; Murphy, S. M.; Seinfeld,  
606 J. H.; Hildebrandt, L.; Donahue, N. M.; DeCarlo, P. F.; Lanz, V. A.; Prévôt, A. S. H.;  
607 Dinar, E.; Rudich, Y.; Worsnop, D. R. Organic Aerosol Components Observed in  
608 Northern Hemispheric Datasets from Aerosol Mass Spectrometry. *Atmos. Chem.*  
609 *Phys.* **2010**, *10* (10), 4625–4641.
- 610 (36) Cleveland, M. J.; Ziemba, L. D.; Griffin, R. J.; Dibb, J. E.; Anderson, C. H.; Lefer,  
611 B.; Rappenglück, B. Characterization of Urban Aerosol Using Aerosol Mass  
612 Spectrometry and Proton Nuclear Magnetic Resonance Spectroscopy. *Atmos.*



- 613 *Environ.* **2012**, *54*, 511–518.
- 614 (37) Shakya, K. M.; Place, P. F.; Griffin, R. J.; Talbot, R. W. Carbonaceous Content and  
615 Water-Soluble Organic Functionality of Atmospheric Aerosols at a Semi-Rural New  
616 England Location. *J. Geophys. Res. Atmos.* **2012**, *117*(3), 1–13.
- 617 (38) Timonen, H.; Carbone, S.; Aurela, M.; Saarnio, K.; Saarikoski, S.; Ng, N. L.;  
618 Canagaratna, M. R.; Kulmala, M.; Kerminen, V.-M.; Worsnop, D. R.; Hillamo, R.  
619 Characteristics, Sources and Water-Solubility of Ambient Submicron Organic  
620 Aerosol in Springtime in Helsinki, Finland. *J. Aerosol Sci.* **2013**, *56*, 61–77.
- 621 (39) Chalbot, M.-C. G.; Brown, J.; Chitranshi, P.; Gamboa da Costa, G.; Pollock, E. D.;  
622 Kavouras, I. G. Functional Characterization of the Water-Soluble Organic Carbon  
623 of Size-Fractionated Aerosol in the Southern Mississippi Valley. *Atmos. Chem.*  
624 *Phys.* **2014**, *14*(12), 6075–6088.
- 625 (40) Paglione, M.; Saarikoski, S.; Carbone, S.; Hillamo, R.; Facchini, M. C.; Finessi, E.;  
626 Giulianelli, L.; Carbone, C.; Fuzzi, S.; Moretti, F.; Tagliavini, E.; Swietlicki, E.;  
627 Stenstrom, K. E.; Prévôt, A. S. H.; Massoli, P.; Canaragatna, M.; Worsnop, D.;  
628 Decesari, S. Primary and Secondary Biomass Burning Aerosols Determined by

- 629 Proton Nuclear Magnetic Resonance ( $^1\text{H}$ -NMR) Spectroscopy during the 2008  
630 EUCAARI Campaign in the Po Valley (Italy). *Atmos. Chem. Phys.* **2014**, *14* (10),  
631 5089–5110.
- 632 (41) Duarte, R. M. B. O.; Matos, J. T. V.; Paula, A. S.; Lopes, S. P.; Ribeiro, S.; Santos,  
633 J. F.; Patinha, C.; da Silva, E. F.; Soares, R.; Duarte, A. C. Tracing of Aerosol  
634 Sources in an Urban Environment Using Chemical, Sr Isotope, and Mineralogical  
635 Characterization. *Environ. Sci. Pollut. Res.* **2017**, *24* (12), 11006–11016.
- 636 (42) Lopes, C.; Abreu, S.; Válega, M.; Duarte, R.; Pereira, M.; Duarte, A. The  
637 Assembling and Application of an Automated Segmented Flow Analyzer for the  
638 Determination of Dissolved Organic Carbon Based on UV-Persulphate Oxidation.  
639 *Anal. Lett.* **2006**, *39* (9), 1979-1992.
- 640 (43) Hertkorn, N.; Kettrup, A. Molecular Level Structural Analysis of Natural Organic  
641 Matter and of Humic Substances by Multinuclear and Higher Dimensional NMR  
642 Spectroscopy. In *Use of Humic Substances to Remediate Polluted Environments:  
643 From Theory to Practice*, Perminova, I. V., Hatfield, K., Hertkorn, N., Eds.; Springer,  
644 2005; pp 391–435.

- 645 (44) Simpson, A. J.; Burdon, J.; Graham, C. L.; Hayes, M. H. B.; Spencer, N.; Kingery,  
646 W. L. Interpretation of Heteronuclear and Multidimensional NMR Spectroscopy of  
647 Humic Substances. *Eur. J. Soil Sci.* **2001**, *52* (3), 495–509.
- 648 (45) Banfi, D.; Patiny, L. Wwww.Nmrdb.Org: Resurrecting and Processing NMR Spectra  
649 On-Line. *Chim. Int. J. Chem.* **2008**, *62* (4), 280–281.
- 650 (46) Morais, E. S.; Silva, N. H. C. S.; Sintra, T. E.; Santos, S. A. O.; Neves, B. M.;  
651 Almeida, I. F.; Costa, P. C.; Correia-Sá, I.; Ventura, S. P. M.; Silvestre, A. J. D.;  
652 Freire, M. G.; Freire, C. S. R Anti-Inflammatory and Antioxidant Nanostructured  
653 Cellulose Membranes Loaded with Phenolic-Based Ionic Liquids for Cutaneous  
654 Application. *Carbohydr. Polym.* **2019**, *206*, 187–197.
- 655 (47) Park, R. J.; Jacob, D. J.; Chin, M.; Martin, R. V. Sources of Carbonaceous Aerosols  
656 over the United States and Implications for Natural Visibility. *J. Geophys. Res.*  
657 **2003**, *108* (D12), 4355.
- 658 (48) Wozniak, A. S.; Bauer, J. E.; Dickhut, R. M. Characteristics of Water-Soluble  
659 Organic Carbon Associated with Aerosol Particles in the Eastern United States.  
660 *Atmos. Environ.* **2012**, *46*, 181–188.

- 661 (49) Schmitt-Kopplin, P.; Gelencsér, A.; Dabek-Zlotorzynska, E.; Kiss, G.; Hertkorn, N.;  
662 Harir, M.; Hong, Y.; Gebefügi, I. Analysis of the Unresolved Organic Fraction in  
663 Atmospheric Aerosols with Ultrahigh-Resolution Mass Spectrometry and Nuclear  
664 Magnetic Resonance Spectroscopy: Organosulfates As Photochemical Smog  
665 Constituents †. *Anal. Chem.* **2010**, *82*(19), 8017–8026.
- 666 (50) Simoneit, B. R. T.; Elias, V. O.; Kobayashi, M.; Kawamura, K.; Rushdi, A. I.;  
667 Medeiros, P. M.; Rogge, W. F.; Didyk, B. M. Sugars - Dominant Water-Soluble  
668 Organic Compounds in Soils and Characterization as Tracers in Atmospheric  
669 Particulate Matter. *Environ. Sci. Technol.* **2004**, *38*(22), 5939–5949.
- 670 (51) Jalava, P. I.; Salonen, R. O.; Pennanen, A. S.; Happonen, M. S.; Penttinen, P.; Hälinen,  
671 A. I.; Sillanpää, M.; Hillamo, R.; Hirvonen, M.-R. Effects of Solubility of Urban Air  
672 Fine and Coarse Particles on Cytotoxic and Inflammatory Responses in RAW 264.7  
673 Macrophage Cell Line. *Toxicol. Appl. Pharmacol.* **2008**, *229*(2), 146–160.
- 674 (52) Chauhan, V.; Breznan, D.; Goegan, P.; Nadeau, D.; Karthikeyan, S.; Brook, J. R.;  
675 Vincent, R. Effects of Ambient Air Particles on Nitric Oxide Production in  
676 Macrophage Cell Lines. *Cell Biol. Toxicol.* **2004**, *20*(4), 221–239.

- 677 (53) Becker, S.; Dailey, L. A.; Soukup, J. M.; Grambow, S. C.; Devlin, R. B.; Huang,  
678 Y.-C. T. Seasonal Variations in Air Pollution Particle-Induced Inflammatory  
679 Mediator Release and Oxidative Stress. *Environ. Health Perspect.* **2005**, *113* (8),  
680 1032–1038.
- 681 (54) Longhin, E.; Pezzolato, E.; Mantecca, P.; Holme, J. A.; Franzetti, A.; Camatini, M.;  
682 Gualtieri, M. Season Linked Responses to Fine and Quasi-Ultrafine Milan PM in  
683 Cultured Cells. *Toxicol. In Vitro* **2013**, *27* (2), 551–559.
- 684 (55) Perrone, M. G.; Gualtieri, M.; Ferrero, L.; Lo Porto, C.; Udisti, R.; Bolzacchini, E.;  
685 Camatini, M. Seasonal Variations in Chemical Composition and in Vitro Biological  
686 Effects of Fine PM from Milan. *Chemosphere* **2010**, *78* (11), 1368–1377.
- 687 (56) Jalava, P. I.; Aakko-Saksa, P.; Murtonen, T.; Happonen, M. S.; Markkanen, A.; Yli-  
688 Pirilä, P.; Hakulinen, P.; Hillamo, R.; Mäki-Paakkanen, J.; Salonen, R. O.;  
689 Jokiniemi, J.; Hirvonen, M.-R. Toxicological Properties of Emission Particles from  
690 Heavy Duty Engines Powered by Conventional and Bio-Based Diesel Fuels and  
691 Compressed Natural Gas. *Part. Fibre Toxicol.* **2012**, *9* (1), 37.
- 692 (57) Uski, O.; Jalava, P. I.; Happonen, M. S.; Torvela, T.; Leskinen, J.; Mäki-Paakkanen, J.;

- 693 Tissari, J.; Sippula, O.; Lamberg, H.; Jokiniemi, J.; Hirvonen, M. R. Effect of Fuel  
694 Zinc Content on Toxicological Responses of Particulate Matter from Pellet  
695 Combustion in Vitro. *Sci. Total Environ.* **2015**, *511*, 331–340.
- 696 (58) Daher, N.; Ruprecht, A.; Invernizzi, G.; De Marco, C.; Miller-Schulze, J.; Heo, J. B.;  
697 Shafer, M. M.; Shelton, B. R.; Schauer, J. J.; Sioutas, C. Characterization, Sources  
698 and Redox Activity of Fine and Coarse Particulate Matter in Milan, Italy. *Atmos.*  
699 *Environ.* **2012**, *49*, 130–141.
- 700 (59) Bachoual, R.; Boczkowski, J.; Goven, D.; Amara, N.; Tabet, L.; On, D.; Leçon-  
701 Malas, V.; Aubier, M.; Lanone, S. Biological Effects of Particles from the Paris  
702 Subway System. *Chem. Res. Toxicol.* **2007**, *20*(10), 1426–1433.
- 703 (60) Bekki, K.; Ito, T.; Yoshida, Y.; He, C.; Arashidani, K.; He, M.; Sun, G.; Zeng, Y.;  
704 Sone, H.; Kunugita, N.; Ichinose, T. PM 2.5 Collected in China Causes  
705 Inflammatory and Oxidative Stress Responses in Macrophages through the  
706 Multiple Pathways. *Environ. Toxicol. Pharmacol.* **2016**, *45*, 362–369.
- 707 (61) Kobayashi, A.; Kang, M.-I.; Watai, Y.; Tong, K. I.; Shibata, T.; Uchida, K.;  
708 Yamamoto, M. Oxidative and Electrophilic Stresses Activate Nrf2 through Inhibition

- 709 of Ubiquitination Activity of Keap1. *Mol. Cell. Biol.* **2006**, *26* (1), 221–229.
- 710 (62) Jalava, P. I.; Happonen, M. S.; Huttunen, K.; Sillanpää, M.; Hillamo, R.; Salonen, R.  
711 O.; Hirvonen, M.-R. Chemical and Microbial Components of Urban Air PM Cause  
712 Seasonal Variation of Toxicological Activity. *Environ. Toxicol. Pharmacol.* **2015**, *40*  
713 (2), 375–387.
- 714 (63) Wang, J.; Huang, J.; Wang, L.; Chen, C.; Yang, D.; Jin, M.; Bai, C.; Song, Y. Urban  
715 Particulate Matter Triggers Lung Inflammation via the ROS-MAPK-NF-KB Signaling  
716 Pathway. *J. Thorac. Dis.* **2017**, *9* (11), 4398–4412.
- 717 (64) Xiao, X.; Wang, R.; Cao, L.; Shen, Z.; Cao, Y. The Role of MAPK Pathways in  
718 Airborne Fine Particulate Matter-Induced Upregulation of Endothelin Receptors in  
719 Rat Basilar Arteries. *Toxicol. Sci.* **2016**, *149* (1), 213–226.
- 720 (65) Longhin, E.; Holme, J. A.; Gualtieri, M.; Camatini, M.; Øvrevik, J. Milan Winter Fine  
721 Particulate Matter (WPM2.5) Induces IL-6 and IL-8 Synthesis in Human Bronchial  
722 BEAS-2B Cells, but Specifically Impairs IL-8 Release. *Toxicol. Vitro.* **2018**, *52* (July),  
723 365–373.
- 724

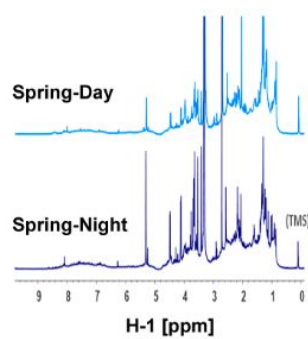
725



726

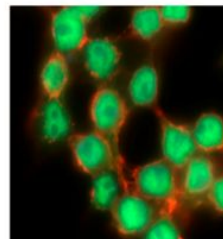
## TOC Art

727

Structural characterization  
of WSOM fraction from PM<sub>2.5</sub>

## Biological activity

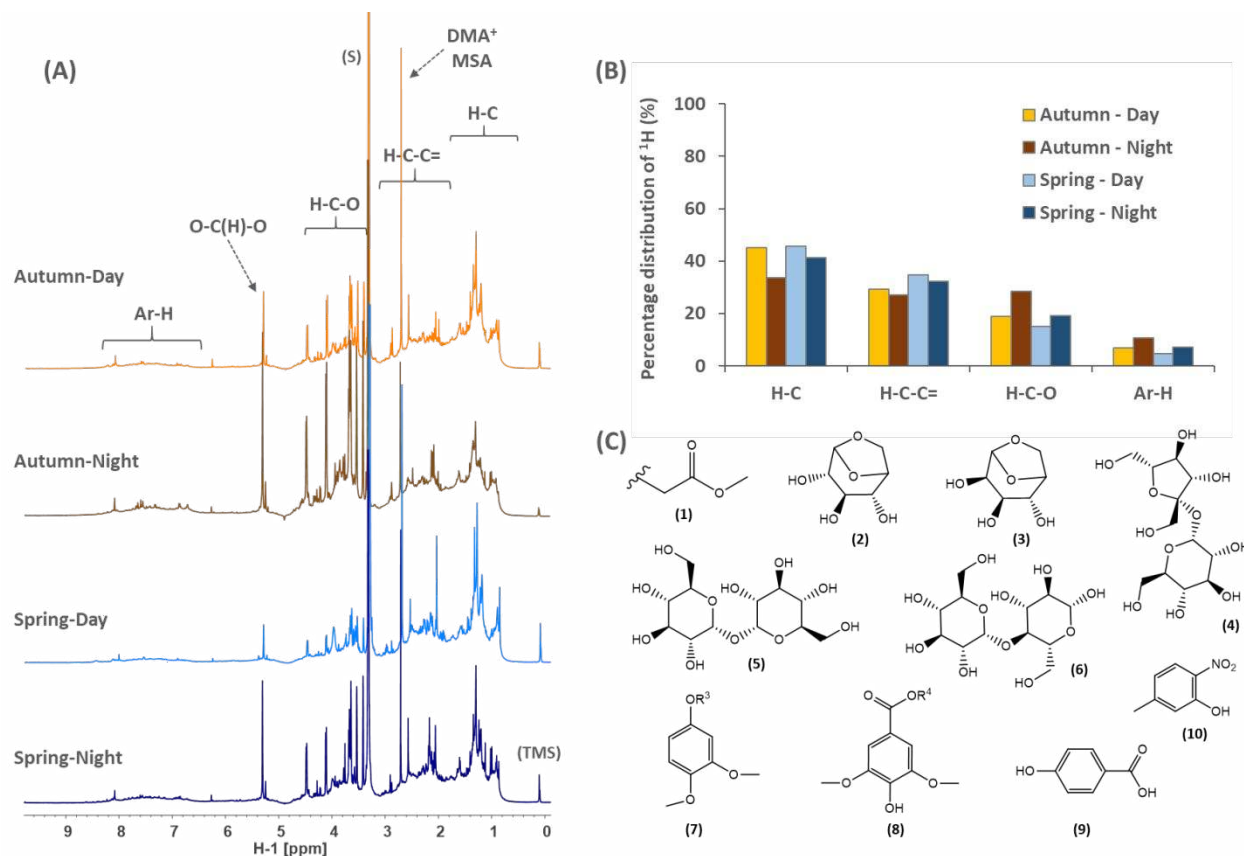
## Raw264.7 Macrophages



- Cytotoxicity
- NO production
- ROS production
- Pro inflammatory gene transcription

728

729



730

731 **Figure 1.** (A) Liquid-state  $^1\text{H}$  NMR spectra of aerosol WSOM samples representative of day and

732 nighttime conditions in Autumn and Spring seasons, (B) percentage distribution of  $^1\text{H}$  NMR in

733 each aerosol WSOM sample, and (C) aliphatic, carbohydrate and aromatic substructures

734 identified in aerosol WSOM collected overnight in Autumn. See Figures S9 and S10 (in SI)

735 for spectral assignments and identity of aromatic substituents ( $\text{R}^3$  and  $\text{R}^4$ ). Four spectral

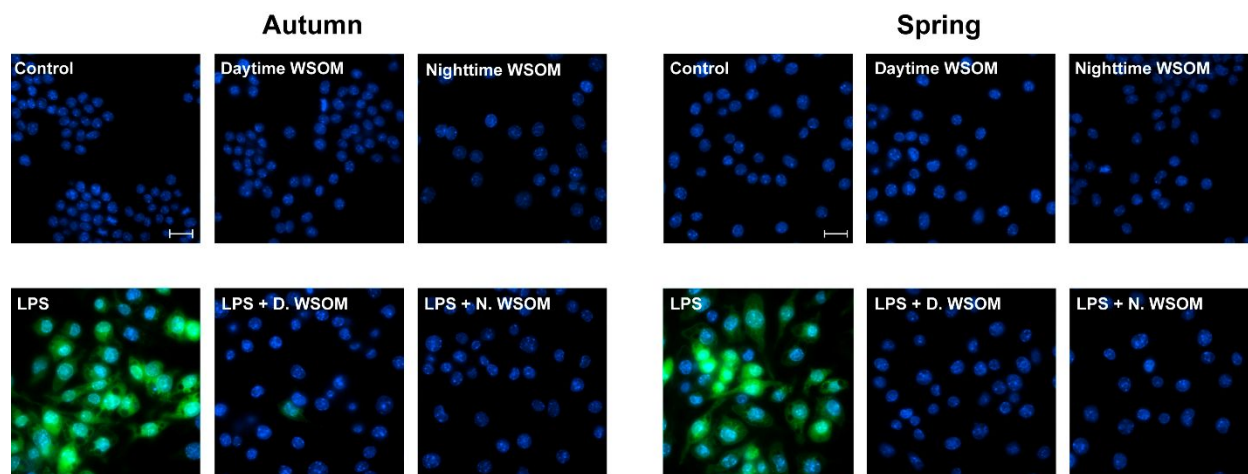
736 regions are identified in  $^1\text{H}$  NMR spectra (A): H-C, H-C-C=, H-C-O, and Ar-H. NMR

737 resonances assigned to dimethylammonium (DMA<sup>+</sup>), methanesulfonic acid (MSA), and

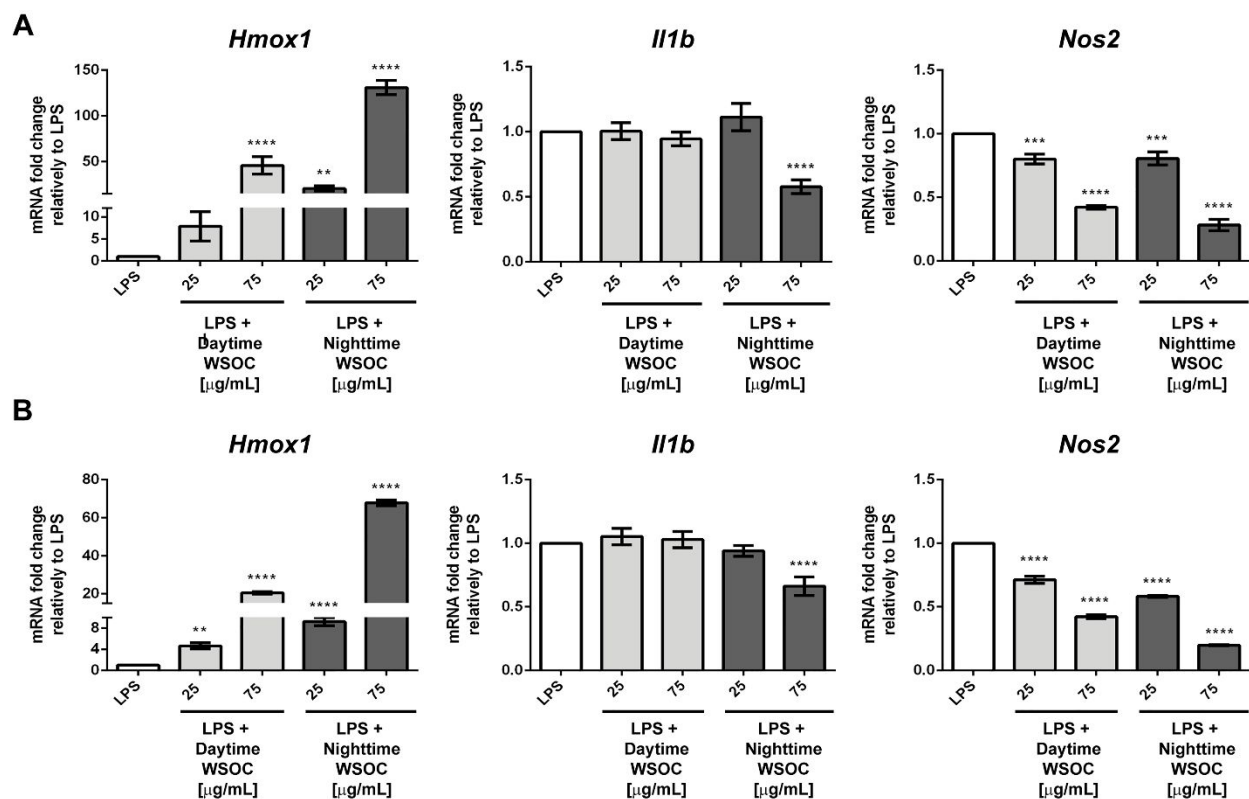
738 protons bound to anomeric carbons [O-C(H)-O] are also identified. Additional resonance

739 signals: solvent (S) – MeOH- $d_4$ , and tetramethylsilane (TMS) – 0.03% (v/v).

740



741  
742 **Figure 2.** Effect of aerosol WSOM samples on macrophage ROS production and modulation of  
743 LPS-induced oxidative stress. Cells were cultured in the indicated conditions and the ROS  
744 production was assessed with H<sub>2</sub>DCFDA (green), a ROS-sensitive fluorescent probe. Hoechst  
745 (blue) was used to label the nuclei. Images representative of different fields were acquired at a  
746 magnification of 63x (scale bar = 20 μm).



748

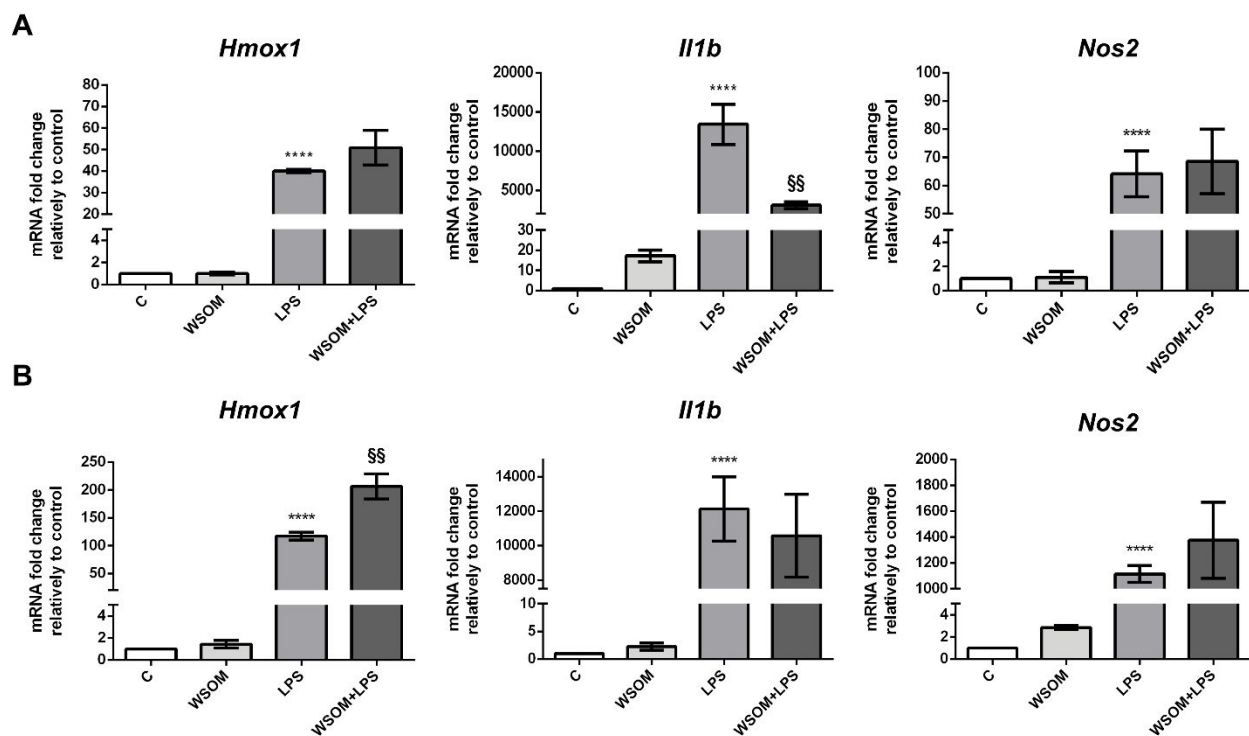
749 **Figure 3.** Effects of aerosol WSOM samples over LPS-induced transcription of *Hmox1*,750 *Il1b* and *Nos2* genes. Cells were exposed to different WSOC concentrations of (A) Autumn

751 (A) and (B) Spring WSOC samples and then stimulated with LPS, followed by mRNA

752 extraction and gene transcription assessment by q-PCR. Data is presented as mRNA fold change

753 relatively to LPS-treated cells and represent the mean  $\pm$  SD from at least 3 independent754 experiments. (\* $p < 0.05$ ; \*\* $p < 0.01$ ; \*\*\* $p < 0.001$ ; \*\*\*\* $p < 0.0001$ : LPS vs WSOM+ LPS).

755



756

757 **Figure 4.** Impact of prolonged exposure to maximal theoretical doses of aerosol WSOM758 samples in the (A) gene transcription and (B) LPS-induced gene transcription of *Hmox1*,759 *Il1b*, and *Nos2*. Cells were exposed for 3 weeks to maximal theoretical quantities of WSOC

760 extracts, followed by mRNA extraction and gene transcription assessment by q-PCR. Data is

761 presented as mRNA fold change relatively to control or to LPS-treated cells and represent the

762 mean  $\pm$  SD from at least 3 independent experiments. [\*\*\*\* $p < 0.0001$ : Control (C) vs treatments;763 §§ $p < 0.01$ : LPS vs WSOM+LPS].

764

765

766 **Table 1.** Ambient concentrations (maximum – minimum; median) of urban PM<sub>2.5</sub>, OC,  
 767 EC, WSOC, and WSOC/OC in each sampling period.

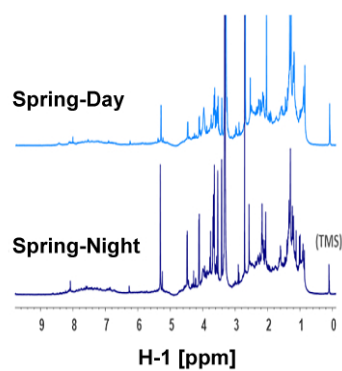
Season	Sampling Period	PM <sub>2.5</sub> (µg m <sup>-3</sup> )	OC (µg C m <sup>-3</sup> )	EC (µg C m <sup>-3</sup> )	WSOC (µg C m <sup>-3</sup> )	WSOC/OC (%)
Autumn	Day	60 – 14; 32	14 – 1.6; 4.1	2.2 – 0.3; 1.3	5.6 – 0.2; 1.3	39 – 12; 34
	Night	75 – 10; 47	20 – 1.5; 14	5.0 – 0.3; 3.0	6.5 – 0.5; 4.7	34 – 29; 33
Spring	Day	30 – 5.1; 21	6.2 – 0.75; 3.3	1.2 – 0.0; 0.4	2.7 – 0.43; 1.1	57 – 32; 42
	Night	29 – 3.2; 22	6.3 – 1.3; 4.3	1.4 – 0.3; 0.9	2.6 – 0.54; 1.6	44 – 35; 41

768

769

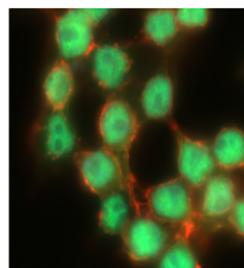
770

### Structural characterization of WSOM fraction from $PM_{2.5}$



### Biological activity

Raw264.7 Macrophages



- Cytotoxicity
- NO production
- ROS production
- Pro inflammatory gene transcription

TOC Art